Journal of Inorganic Biochemistry 155 (2016) 92–100

Contents lists available at ScienceDirect

Journal of Inorganic Biochemistry

journal homepage: www.elsevier.com/locate/jinorgbio

Synthesis of platinum complexes with 2-(5-perfluoroalkyl-1,2,4-oxadiazol-3yl)-pyridine and 2-(3-perfluoroalkyl-1-methyl-1,2,4-triazole-5yl)-pyridine ligands and their in vitro antitumor activity

Simona Rubino *, Ivana Pibiri *, Cristina Costantino, Silvestre Buscemi, Maria Assunta Girasolo, Alessandro Attanzio, Luisa Tesoriere

Dipartimento di Scienze e Tecnologie Biologiche, Chimiche e Farmaceutiche (STEBICEF), Università di Palermo, Viale delle Scienze Ed. 17, Parco d'Orleans, 90128 Palermo, Italy

ARTICLE INFO

Article history:
Received 20 July 2015
Received in revised form 12 November 2015
Accepted 17 November 2015
Available online 1 December 2015

Keywords:
Mononuclear platinum complexes
Perfluoroalkyl heterocyclic ligands
Antitumor activity

ABSTRACT

Five new mononuclear Pt(II) complexes with 5-perfluoroalkyl-1,2,4-oxadiazolyl-pyridine and 3-perfluoroalkyl-1,2,4-triazolyl-pyridine ligands are reported. The ligands 2-(5-perfluoroheptyl-1,2,4-oxadiazole-3yl)-pyridine **(pfhop)**, 2-(5-perfluoropropyl)-1,2,4-oxadiazole-3yl)-pyridine **(pfpop)**, 2-(3-perfluoroheptyl-1-methyl-1,2,4-triazole-5yl)-pyridine **(pfhtp)**, 2-(3-perfluoropropyl-1-methyl-1,2,4-triazole-5yl)-pyridine **(pfptp)** and their complexes $[PtCl_2(pfhop)_2]\cdot 1.5$ DMSO (**2a**), $[PtCl_2(pfpop)_2]\cdot 1.5$ DMSO (**3a**), $[PtCl_2(pfhtp)_2]\cdot 1.5$ DMSO (**4a**), $PtCl_2(pfhtp)$ (**4b**), $[PtCl_2(pfptp)_2]\cdot 1.5$ DMSO (**5a**) have been synthesized and structurally characterized. The complexes **2a, 3a, 4a** and **5a** have the same chemical environment of Pt(II) where $PtCl_2$ moieties coordinate two molecules of ligand via N1 atom of pyridine in the case of **pfhop** and **pfpop,** and N2 atom of 1,2,4-triazole in the case of **pfhtp** and **pfptp**. For **4b, pfhtp** behaves as bidentate ligand, coordinating Pt(II) ion via N4 atom of triazole and N1 atom of pyridine. All complexes have been tested in vitro by 3-(4,5-dimethyl-2-thiazolyl)bromide-2,5-diphenyl-2 H-tetrazolium (MTT) test on four tumor cell lines MCF-7 (human breast cancer), HepG2 (human hepatocellular carcinoma), HCT116 (human colorectal carcinoma). Compounds **2a** and **4b** showed a dose-dependent anti-proliferative effect against the three tumor cell lines whereas did not affect viability of intestinal normal-like differentiated Caco-2 cells. The cell death of HepG2, MCF-7 and HCT116 induced by the compounds, was considered to be apoptotic by measuring the exposure of phosphatidylserine to the outer membrane and observing the typical apoptotic morphological change by acridine orange (AO)/ethidium bromide (EB) staining.

1. Introduction

In the last decades, the successful application of cisplatin antitumor therapies has triggered considerable interest in the search for more affective cisplatin analogs. Many efforts have been dedicated to explain the factors related to the anticancer activity of cisplatin and different platinum compounds [1,2] and although the molecular mechanistic studies of cisplatin and analogs have been largely developed, the cellular response to these compounds is still poorly understood [3,4].

Several studies have been conducted with common goals, such as the design of new metal complexes that keep active against resistant cell lines, with a large spectrum of anticancer activity and also with a lower toxicity than cisplatin [5]. However, the cross resistance and severe side effects of platinum drugs, such as nephrotoxicity, have limited their clinical application. In the past years, successful approaches have been employed to solve these drawbacks, combining platinum-based drugs with some other active pharmacophore so that a synergic action can be obtained [6]. Oxadiazole and triazole have been recently used for complexation of metal such as copper, nickel [7], palladium [8] and platinum [9]; 1,2,4-oxadiazoles have been widely studied for their chemistry [10–12], these heterocycles have gained attention for their pharmaceutical properties, and additionally, the presence of the fluorinated moiety opens the way to new fluorine-induced activity with respect to corresponding non-fluorinated systems [13–16] and application in materials [17–21]. In particular, a series of Pt(II) complexes with 1,2,4-oxadiazole derivatives as ligands have shown cytotoxic activity towards human ovarian cancer, and also in colon and testicular cancer cell lines.

Abbreviations: AO, acridine orange; DMF, dimethylformamide; DMSO, dimethylsulfoxide; EB, Ethidium Bromide; FACS, Fluorescence-Activated Cell Sorting; FBS, Fetal Bovine Serum; FITC, Fluorescein isothiocyanate; GC/MS, Gas Chromatography/Mass Spectrometry; HRMS, High Resolution Mass; MTT, 3-(4,5-dimethyl-2-thiazolyl)bromide-2,5-diphenyl-2 H-tetrazolium; PBS, phosphate buffer; PI, propidium iodide; PS, phosphatidylserine; RPMI, Roswell Park Memorial Institute; TLC, Thin Layer Chromatography; TMS, tetramethylsilane.

* Corresponding authors.
E-mail addresses: simona.rubino@unipa.it (S. Rubino), ivana.pibiri@unipa.it (I. Pibiri).

http://dx.doi.org/10.1016/j.jinorgbio.2015.11.020
0162-0134/

This activity has been attributed to their DNA-binding properties [22]. In the same way, triazole rings have been widely studied as bioactive moieties [23] and also have been used as ligands in order to synthesize cytotoxic platinum, palladium and organotin(IV) complexes [24–27].

In this paper, we report the synthesis and characterization of new platinum complexes and the synthesis of the new ligands: **pfhop, pfpop, pfhtp** and **pfptp**. In **2a** and **3a** complexes, the coordination of 2-(5-perfluoroalkyl-1,2,4-oxadiazol-3yl)-pyridine ligands involve the N1 atom of pyridine, acting as monodentate ligand, as already observed in the literature for Cu(II), Co(II) and Ni(II) complexes with 2,5-bis(2-pyridyl)-1,3,4-oxadiazolyl-pyridine [7]. The coordination of Pt(II) ion to the 2-(3-perfluoroalkyl-1-methyl-1,2,4-triazole-5yl)-pyridine ligands for **4a** and **5a** complexes, occurs via N2 atoms of two 1,2,4-triazole moieties as already observed in the literature for azole-bridged dinuclear platinum(II) complexes [24]. On the contrary, in the case of **4b,** only one molecule of 1,2,4-triazolyl-pyridine is coordinated to Pt(II) ion via N4 atom of triazole moiety and N1 atom of pyridine respectively, where the ligand is bidentate as reported in literature with Pt(II) and Pd(II) ions [8]. Cytotoxicity in vitro of the synthesized cisplatin analogs was evaluated by MTT test on three tumor human cell lines: HepG2, MCF-7 and HTC116. The calculated IC_{50} values of **2a** and **4b** complexes show that antiproliferative activity of both the cisplatin analogs was comparable to that observed with cisplatin, being **2a** significantly more effective than **4b** against all the selected cancer cells. Mechanism of the anti-proliferative effect of **2a** and **4b** was investigated by double staining with propidium iodide (PI) and Annexin V-Fluorescein isothiocyanate (FITC) followed by cytofluorimetric analysis and shows that **2a** and **4b** complexes induce a clear shift of viable cells towards early apoptosis in HepG2 and HCT116 or towards late apoptosis in MCF-7 cells.

2. Experimental

2.1. General methods

All solvents and reagents were obtained from commercial sources (Sigma-Aldrich). *Cis*-[$PtCl_2(DMSO)_2$] [28] and N-hydroxypicolinamidine **1** (95% yields, m.p. 116–118 °C) were synthesized according to previously reported method [29]. Syntheses were performed with exclusion of moisture and direct light. Elemental analysis for C, H, N, were performed at the Laboratorio di Microanalisi (University of Padova, Italy); chlorine was determined by potentiometric titration with standard silver nitrate after combustion in pure oxygen according to Schöniger [30]. The percentage of platinum in the complexes has been measured by a Perkin–Elmer 372 atomic absorption spectrometer against the appropriate standards. IR spectra (Nujol) were registered with a Shimadzu FTIR-8300 instrument. ^{1}H NMR spectra were recorded on a Bruker 300 Avance spectrometer, operating at 300 MHz, with tetramethylsilane (TMS) as an internal standard. The molar conductivities for all complexes were determined in DMSO at 10^{-3} M at 25 °C with a Crison GLP 31 Model Conductometer. Gas Chromatography/Mass Spectrometry (GC/MS) spectra were determined with a Shimadzu QP-2010 instrument. High Resolution Mass (HRMS) were determined by Agilent Technologies 6540 UHD Accurate-Mass Q-TOF LC/MS instrument. Melting points were determined on a Kofler plate with Reichart–Thermovar hotstage apparatus and are uncorrected. Flash chromatography was performed by using silica gel (Merck, 0.040–0.063 mm) and mixtures of ethyl acetate and petroleum (fraction boiling in the range 40–60 °C) in various ratios.

2.2. Synthesis of ligands

2.2.1. General method of synthesis of 1,2,4-oxadiazolyl-pyridines

The synthetic approach for the preparation of substituted 1,2,4-oxadiazoles derivatives is shown in Scheme 1. N-hydroxypicolinamidine **1** (1 g) was dissolved in toluene (60 ml) in a round-bottomed flask, and then pyridine (1 ml) and appropriate acyl chloride (1.2 equivalent) were added.

The reaction mixture was allowed to reflux for 6–8 h and was monitored by thin layer chromatography (TLC) until the reaction was complete. The solvent was removed under vacuum, and then the residue was added with water (60 ml) and extracted with ethyl acetate (50 ml × 3). The organic layer was dried over anhydrous Na_2SO_4, and solvent was removed under vacuum. The residue was purified through silica gel column chromatography using a mixture of ethyl acetate and petroleum as eluent to afford the desired oxadiazolyl-pyridine [31–32].

2.2.2. 2-(5-perfluoroheptyl-1,2,4-oxadiazol-3-yl)-pyridine (pfhop) (2)

The compound **2** was prepared following the general procedure, by reacting N-hydroxypicolinamidine **1** (1.015 g, 7.293 mmol) and pentadecafluorooctanoyl chloride (2.170 ml, 8.752 mmol). The product was obtained as a yellow solid in 70% yield, m.p. 74–76 °C. ^{1}H NMR (CD_3CN, 300 MHz) δ ppm: 8.79 (d, J = 4.5 Hz, 1H, Pyridyl), 8.14 (d, J = 7.8 Hz, 1H, Pyridyl), 8 (dt, J = 1.82 e 7.8 Hz, 1H, Pyridyl), 7.6 (dd, J = 4.76 e 7.8 Hz, 1H, Pyridyl); MS *m/z* (%) 515 (M^+, 100), 166 (25), 120 (90), 78 (90), 51 (20). HRMS $C_{14}H_4F_{15}N_3O$ [M + H] calculated 516.0187, found 516.0182.

2.2.3. 2-(5-perfluoropropyl-1,2,4-oxadiazol-3-yl)-pyridine (pfpop) (3)

Compound **3** was prepared following the general procedure by reacting N-hydroxypicolinamidine **1** (1.009 g, 7.250 mmol) and heptafluorobutyryl chloride (1.299 ml, 8.700 mmol). The product was obtained as a yellow solid in 88% yield. m.p. 87–90 °C. ^{1}H NMR (DMSO-d_6, 300 MHz,) δ ppm: 8.85 (dd, J = 2.5 e 5.7 Hz, 1H, Pyridyl), 8.18 (dd, J = 1.8 e 8 Hz, 1H, Pyridyl), 8.10 (dt, J = 1.6 e 7.3 Hz, 1H, Pyridyl), 7.72 (dt, J = 4.6 e 6.8 Hz, 1H, Pyridyl); MS *m/z* (%) 315 (M^+, 100), 285 (15), 120 (75), 78 (90), 69 (20), 51 (25). HRMS $C_{10}H_4F_7N_3O$ [M + H] calculated 316.0315, found 316.0319.

2.2.4. General procedure for the synthesis of 1,2,4-triazoles

The synthetic approach for the preparation of substituted 1,2,4-triazoles derivatives is shown in Scheme 1. To a sample of oxadiazolyl–pyridine (1.5 mmol) in dry dimethylformamide (DMF) (2 ml) an excess of 99% methyl hydrazine (7.5 mmol) was added and the mixture was left at room temperature for 1 h. After dilution with water and extraction with ethyl acetate, the combined extracts were dried over Na_2SO_4 and the solvent was removed under vacuum. The residue was purified through silica gel column chromatography using a mixture of ethyl acetate and petroleum as eluent to afford the desired triazolyl–pyridine [32].

2.2.5. 2-(3-perfluoroheptyl-1-methyl-1,2,4-triazole-5-yl)-pyridine (pfhtp) (4)

Compound **4** was prepared starting by 2-(5-Perfluoroheptyl-1,2,4-oxadiazol-3-yl)-pyridine **2** (1.011 g, 1.963 mmol). The product was extracted with ethyl acetate, purified through silica gel column chromatography using petroleum/ethyl acetate in ratio 6/1, affording a white crystalline solid in 70% yield; m.p. 49–51 °C. ^{1}H NMR (DMSO-d_6, 300 MHz,) δ ppm: 8.80 (d, J = 3.75 Hz, 1H, Pyridyl), 8.17 (d, J = 6.75 Hz, 1H, Pyridyl), 8.05 (dt, J = 1.25 e 6.5 Hz, 1H, Pyridyl), 7.67 (m, J = 4 e 6.25 Hz, 1H, Pyridyl), 4.39 (s, 3H, Me); MS *m/z* (%) 528 (M^+,40), 527 (95), 209 (15), 159 (65), 133 (60), 106 (25), 105 (1000), 78 (35). HRMS $C_{15}H_7F_{15}N_4$ [M + H] calculated 529.0504, found 529.0510.

2.2.6. 2-(3-perfluoropropyl-1-methyl-1,2,4-triazole-5-yl)-pyridine (pfptp) (5)

Compound **5** was prepared starting by 2-(5-Perfluoropropyl-1,2,4-oxadiazol-3-yl)-pyridine **3** (1.855 g, 5.655 mmol). The product was extracted with ethyl acetate, chromatographed with light petroleum/ethyl acetate in ratio 6/1, affording an oil in 78% yield; ^{1}H NMR (DMSO-d_6, 300 MHz) δ ppm: 8.79 (d, J = 4.6 Hz, 1H, Pyridyl), 8.16 (d, J = 7.3 Hz, 1H, Pyridyl), 8.05 (dt, J = 1.7 e 7.3 Hz, 1H, Pyridyl), 7.61 (dd, J = 4.4 e

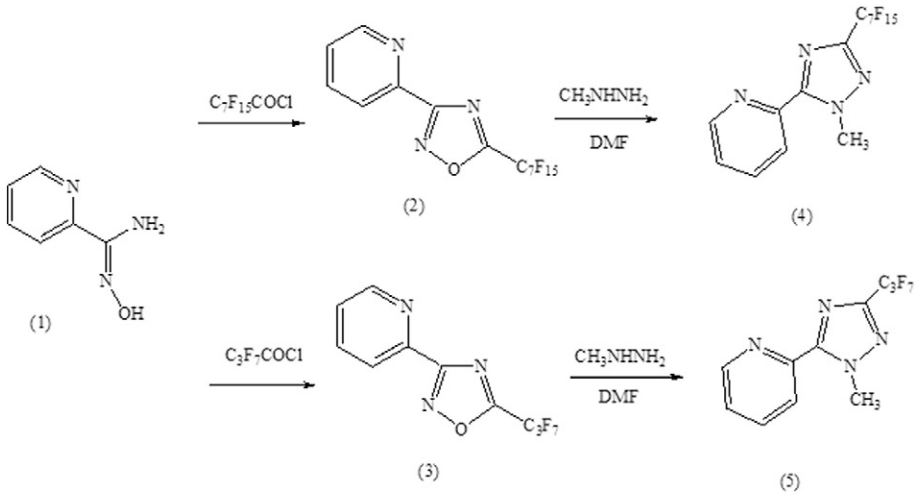

Scheme 1. Synthesis of the ligands 2–5.

7 Hz, 1H, Pyridyl), 4.39 (s, 3 H, Me). MS *m/z* (%) 328 (M^+, 35), 327 (85), 159 (40), 133 (50), 105 (100), 78 (40). HRMS $C_{11}H_7F_7N_4$ [M + H] calculated 329.0631, found 329.0635.

2.3. General procedures of synthesis of complexes (**2a**), (**3a**), (**4a**), (**5a**)

Cis-[$PtCl_2(DMSO)_2$] (0.174 g, 0.4 mmol) and the ligands **2**, **3**, **4, 5** respectively, were dissolved in 25 ml of chloroform under 1:1 stoichiometry. The resulting solution was stirred for 24 h at 40 °C. The yellow solids were filtered, washed with chloroform and dried in vacuo over P_4O_{10}. The synthesis of the complexes can be summarized in Scheme 2.

2.3.1. [$PtCl_2(pfhop)_2$]·1.5 DMSO (**2a**)

The complex **2a** was prepared following the general procedure. Yield 60%. Anal. Calc. for ($C_{30}H_{14}N_6O_3SF_{30}PtCl_2$)·0.5 DMSO: C, 26.34; H, 1.21;

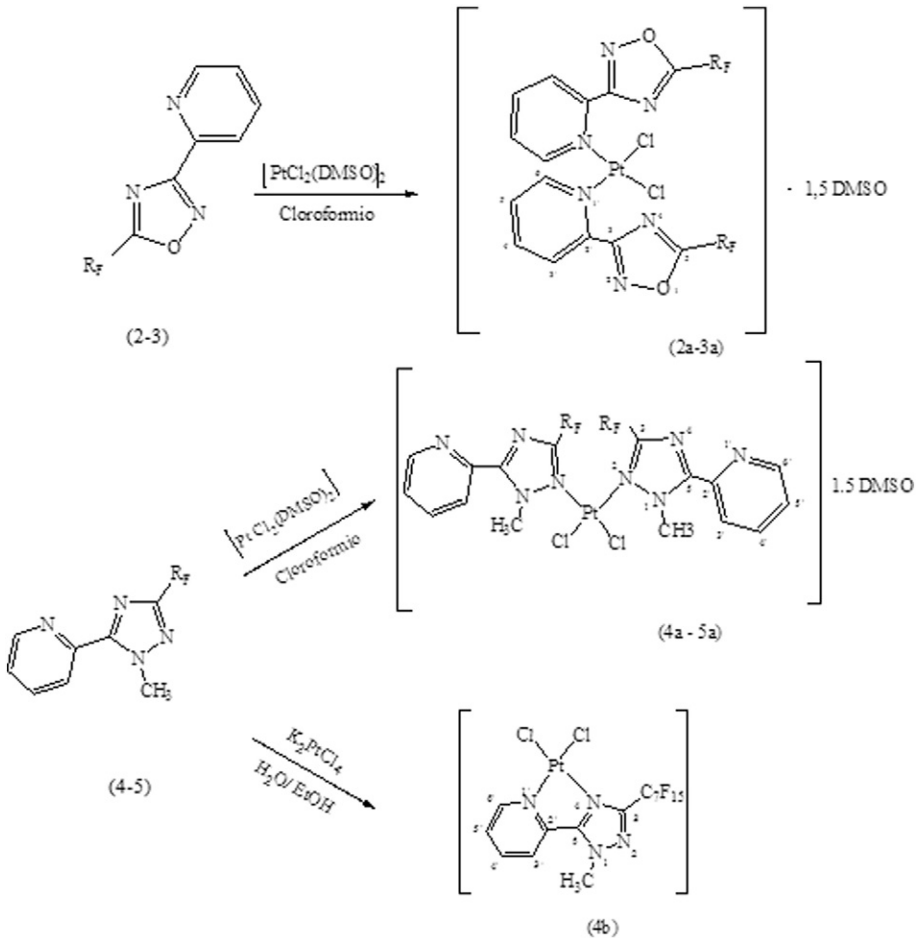

Scheme 2. Synthesis of platinum complexes: $R_F = C_7F_{15}$ (2a, 4a, 4b); $R_F = C_3F_7$ (3a, 5a).

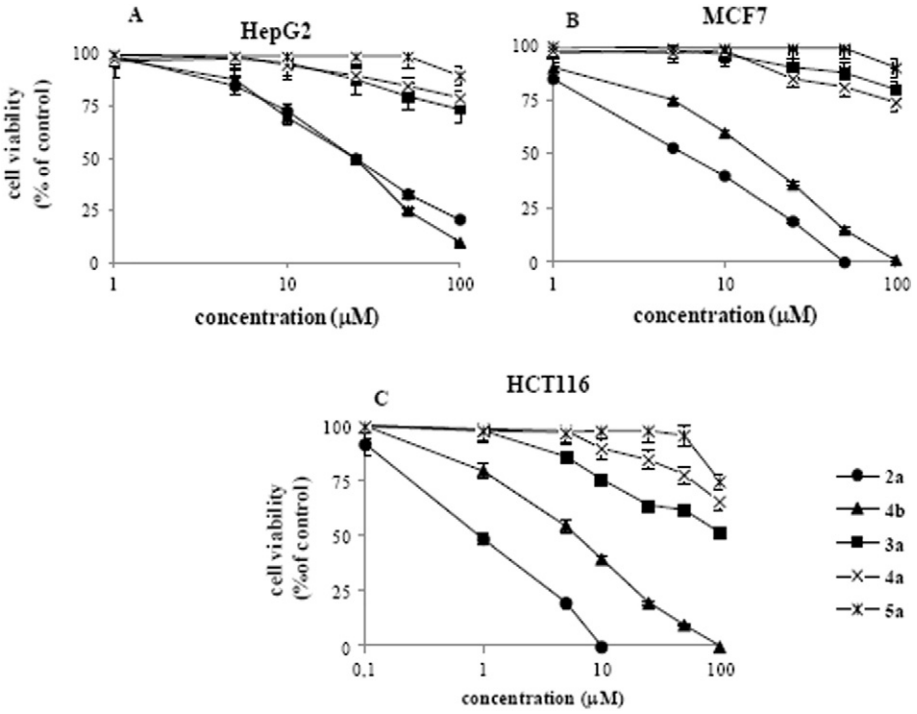

Fig. 1. Cytotoxic effect of the synthesized cisplatin analogs on Hep-G2 cells (A), MCF-7 (B) or HCT116 (C) cells as assessed by MTT. Cell monolayers were incubated for 24 h in the absence (control) or in the presence of the compounds at the indicated concentrations and cell viability was assessed by MTT test as reported in *Experimental*. Results are indicated as the percentage of viable cells with respect to untreated controls. Values are the mean ± SD of three separate experiments carried out in triplicate.

N, 5.95; S, 3.40; Cl, 5.02; Pt, 13.80%. Found: C, 26.74; H, 1.09; N, 5.66; S, 3.00; Cl, 5.03; Pt, 13.90%. Melting point: >350 °C (decomp.). Λ_M = 15.30 Ω^{-1} cm^2 mol^{-1} (indicative of neutral complex) [33]. IR (cm^{-1}) for free ligand: 1591 ν(CH═N), 1214–1150 ν(C–F), and for the complex 1534 ν(CH═N), 1628 ν(C═N), 1241–1144 ν(C–F), 1023 ν(S═O of non-coord. DMSO), 342 e 326 ν(Pt–Cl) and 279, 256 ν(Pt–N). ^{1}H NMR for the

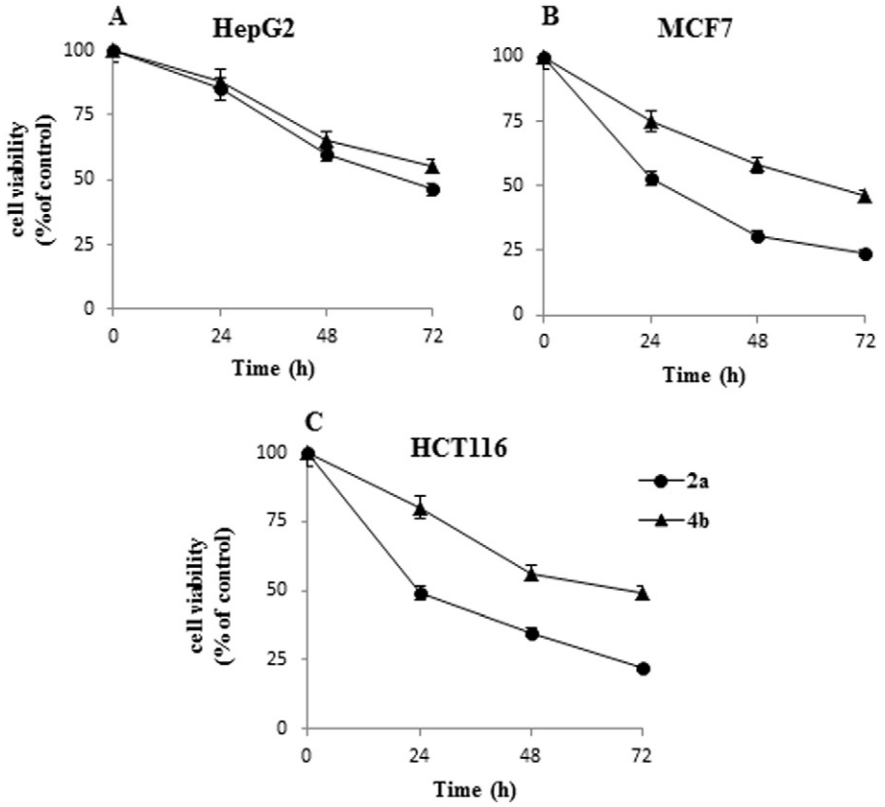

Fig. 2. Inhibitory effect of the complexes **2a** or **4b** on the growth of HepG2 (A), MCF-7 (B) or HCT116 (C) cells. Cell monolayers were incubated for the indicated times in the absence (control) or in the presence of **2a** or **4b** at 1 μM (HCT116) or in the presence of **2a** or **4b** at 5 μM (HepG2 and MCF-7). Cell viability was assessed by MTT test as reported in *Experimental*. Results are indicated as the percentage of viable cells with respect to untreated controls. Values are the mean ± SD of three separate experiments carried out in triplicate.

complex (CD_3CN, 300 MHz) δ ppm: 9.50 (d, 2H, $C_6HC_{6'}H$), 8.25 (dt, 2H, $C_5HC_{5'}H$), 7.78 (d, 2H, $C_3HC_{3'}H$), 7.68 (m, 2H, $C_4HC_{4'}H$), 2.65 (non-coord. DMSO); $^3J_{C3'HC4'H} = 9.5$ Hz; $^3J_{C6'HC5'H} = 5.8$ Hz; $^3J_{C5'HC4'H} = 2.1$ Hz.

*2.3.2. $[PtCl_2(pfpop)_2]\cdot 1.5$ DMSO (**3a**)*

The complex **3a** was prepared following the general procedure. Yield 60%. Anal. Calc. for $(C_{22}H_{14}N_6O_3F_{14}PtCl_2S)\cdot 0.5$ DMSO: C, 27.26; H, 1.69; N, 8.29; S, 4.75; Cl, 7.00; Pt, 19.25%. Found: C, 27.60; H, 1.63; N, 8.44; S, 4.82; Cl, 6.60; Pt, 18.95%. Melting point: >350 °C (decomp.). Λ_M = 19.70 Ω^{-1} cm^2 mol^{-1} (indicative of neutral complex) [33]. IR (cm^{-1}) for free ligand: 1590 ν(CH═N), 1223–1159 ν(C–F) and for the complex 1590, 1535 ν(CH═N), 1631 ν(C═N) 1216–1157 ν(C–F), 333 e 320 ν(Pt–Cl), 279, 257 ν(Pt–N). ^{1}H NMR for the complex (DMSO, 300 MHz) δ ppm: 9.07 (d, 2H, $C_6HC_{6'}H$), 8.34 (dt, 2H, $C_5HC_{5'}H$), 8.56 (d, 2 H, $C_3HC_{3'}H$), 8.15 (m, 2 H, $C_4HC_{4'}H$), 2.53–2.51 (s, non-coord. DMSO); $^3J_{C3'HC4'H} = 9.5$ Hz; $^3J_{C6'HC5'H} = 5.8$ Hz; $^3J_{C5'HC4'H} = 2.1$ Hz.

*2.3.3. $[PtCl_2(pfhtp)_2]\cdot 1.5$ DMSO (**4a**)*

The complex **4a** was prepared following the general procedure. Yield 60%. Anal. Calc. for $(C_{32}H_{20}N_8F_{30}PtCl_2SO)\cdot 0.5$ DMSO: C, 27.53; H, 1.61; N, 7.78; S, 3.34; Cl, 4.93; Pt, 13.55%. Found: C, 27.93; H, 1.40; N, 8.06; S, 3.30; Cl, 5.00; Pt, 13.15%. Melting point: >350 °C (decomp.). Λ_M = 3.30 Ω^{-1} cm^2 mol^{-1} (indicative of neutral complex) [33]. IR (cm^{-1}) for free ligand: 1590 ν(CH═N), 1240–1147 ν(C–F) and for the complex 1591 ν(CH═N), 1242–1147 ν(C–F), 1037 ν(S═O), 338, 312 ν(Pt–Cl), 277 ν(Pt–N). ^{1}H NMR for the complex (DMSO, 300 MHz) δ ppm: 8.85 (d, 2H, $C_6HC_{6'}H$), 8.22 (d, 2H, $C_3HC_{3'}H$), 8.11 (t, 2 H, $C_5HC_{5'}H$), 7.68 (t, 2H, $C_4HC_{4'}H$), 4.44 (s, 3H, Me), 2.61–2.57 (s, non-coord. DMSO); $^3J_{C6'HC5'H} = 5.2$ Hz; $^3J_{C4'HC3'H} = 9.3$ Hz, $^3J_{C5'HC4'H} = 6.0$ Hz.

*2.3.4. $PtCl_2(pfhtp)$ (**4b**)*

An aqueous solution of K_2PtCl_4 (0.554 g, 1.05 mmol) was added dropwise in stirring to a solution of **4** (0.436 g, 1.05 mmol) in ethanol (25 ml) at 40 °C. A red solid was filtered and washed with water, ethanol and diethyl ether and dried in vacuo over P_4O_{10}. Yield 60%. Anal. Calc. for $C_{15}N_4H_7F_{15}PtCl_2$: C, 22.68; H, 0.89; N, 7.05; Cl, 8.93; Pt, 24.56%. Found: C, 23.00; H, 0.97; N, 7.23; Cl, 8.46; Pt, 24.90%. Melting point: >350 °C (decomp.). Λ_M = 1.75 Ω^{-1} cm^2 mol^{-1} (indicative of neutral complex) [33]. IR (cm^{-1}) for the complex 1592 ν(CH═N), 1658 ν(C═N), 1242–1147 ν(C–F), 343, 320 ν(Pt–Cl), 272 ν(Pt–N). ^{1}H NMR for the complex (DMSO, 300 MHz) δ ppm: 8.85 (d, 1H, $C_6HC_{6'}H$), 8.22 (d, 1H, $C_3HC_{3'}H$), 8.11 (dt, 1H, $C_5HC_{5'}H$), 7.68 (dt, 1H, $C_4HC_{4'}H$), 4.44 (s, 3H, Me); $^3J_{C6'HC5'H} = 5.4$ Hz; $^3J_{C4'HC3'H} = 9.3$ Hz, $^3J_{C5'HC4'H} = 1.9$ Hz.

*2.3.5. $[PtCl_2(pfptp)_2]\cdot 1.5$ DMSO (**5a**)*

The complex **5a** was prepared following the general procedure. Yield 80%. Anal. Calc. for $(C_{24}H_{20}N_8F_{14}PtCl_2SO)\cdot 0.5$ DMSO: C, 28.88; H, 2.23; N, 10.78; S, 4.63; Cl, 6.82; Pt, 18.77%. Found: C, 29.28; H, 1.85; N, 11.18; S, 4.27; Cl, 6.42; Pt, 19.17%. Melting point: >350 °C (decomp.). Λ_M = 1.47 Ω^{-1} cm^2 mol^{-1} (indicative of neutral complex) [33]. IR (cm^{-1}) for free ligand: 1590 ν(CH═N), 1242–1147 ν(C–F), and for the complex 1649–1665 ν(C═N), 1592 ν(CH═N), 1242–1147 ν(C–F), 1032 ν(S═O), 333, 322 ν(Pt–Cl), 271 ν(Pt–N). ^{1}H NMR for the complex (DMSO, 300 MHz) δ ppm: 8.80 (d, 2H, $C_6HC_{6'}H$), 8.19 (d, 2H, $C_3HC_{3'}H$), 8.03 (t, 2H, $C_5HC_{5'}H$), 7.62 (t, 2H, $C_4HC_{4'}H$), 4.39 (s, 3H, CH_3), 2.52–2.55 (s, non-coord. DMSO); $^3J_{C6'HC5'H} = 5.2$ Hz; $^3J_{C4'HC3'H} = 9.3$ Hz; $^3J_{C5'HC4'H} = 6.0$ Hz.

2.4. Biological studies

2.4.1. Viability assay in vitro

Synthesized platinum(II) complexes and relative ligands were dissolved in dimethylsulfoxide (DMSO) and then diluted in culture medium so that the effective DMSO concentration did not exceed 0.1%. HepG2, MCF-7 and HTC116 and Caco-2 (human colorectal carcinoma) cell lines were purchased from American Type Culture Collection, Rockville, MD, USA. All of them were grown in Roswell Park Memorial Institute (RPMI) medium supplemented with L-glutamine (2 mM), 10% fetal bovine serum (FBS), penicillin (100 U/ml), streptomycin (100 μg/ml) and gentamicin (5 μg/ml). HepG2 culture medium also contained sodium pyruvate (1.0 mM). Cells were maintained in log phase by seeding twice a week at a density of 3×10^8 cells/l in humidified 5% CO_2 atmosphere, at 37 °C. In all experiments, cells were made quiescent through overnight incubation before the treatment with the compounds or vehicle alone (control cells) whereas Caco-2 cells were treated 15 days after confluence, at which time the cells are differentiated in normal intestinal-like cells [34]. No differences were found between cells treated with DMSO 0.1% and untreated cells in terms of cell number and viability.

Table 1
Calculated IC_{50} (μM) values for anti-proliferative activity of **2a** and **4b** cisplatin derivatives against different human cell lines.

$IC_{50} \pm SD$ (μM)			
	HepG2	MCF-7	HCT 116
2a	20.2 ± 1.8	4.0 ± 0.2	1.1 ± 0.06
4b	24.8 ± 2.0	18.5 ± 1.1	8.3 ± 0.7
Cisplatin	50.0 ± 3.1	8.1 ± 0.5	9.1 ± 0.8

Values are the mean ± SD of three separate experiments carried out in triplicate.

Cytotoxic activity of the platinum(II) complexes against human tumor cell lines (HepG2, MCF-7 and HCT116) and intestinal-like differentiated cells (Caco2) was determined by the MTT colorimetric assay based on the reduction of 3-(4,5-dimethyl-2-thiazolyl)bromide-2,5-diphenyl-2H-tetrazolium to purple formazan by mitochondrial dehydrogenases of living cells. This method is commonly used to illustrate inhibition of cellular proliferation. Monolayer cultures were treated for 24 h with various concentrations (0.1–100 μM) of the drugs. Cisplatin and ligands were used for comparison. Briefly, all cell lines were seeded at 2×10^4 cells/well in 96-well plates containing 200 μl RPMI. When appropriated, cells were washed with fresh medium and incubated with the compounds in RPMI. After 24 h incubation, cells were washed, and 50 μl FBS-free medium containing 5 mg/ml MTT were added. The medium was discarded after 2 h incubation at 37 °C by centrifugation, and formazan blue formed in the cells was dissolved in DMSO. The absorbance, measured at 570 nm in a microplate reader (Bio-RAD, Hercules, CA), of MTT formazan of control cells was taken as 100% of viability. IC_{50} value for each

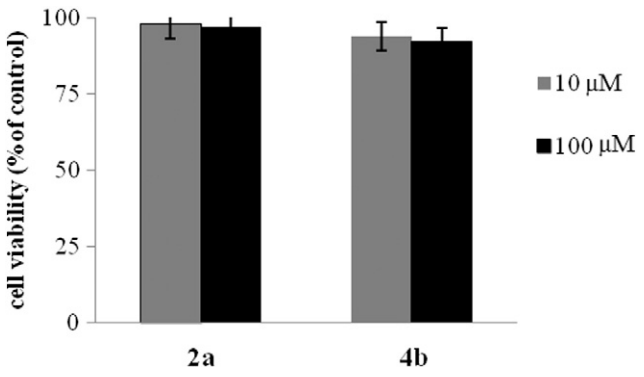

Fig. 3. Effect of the complexes **2a** or **4b** on viability of intestinal normal-like differentiated Caco-2 cells. Cell monolayers were incubated for 24 h in the absence (control) or in the presence of the compounds at the indicated concentrations and cell viability was assessed by MTT test as reported in *Experimental*. Results are indicated as the percentage of viable cells with respect to untreated controls. Values are the mean ± SD of two separate experiments carried out in triplicate.

Table 2
Cell survival of tumor cells treated for 24 h with the ligands **2** and **4,** relative to vehicle control.

Ligand	HepG2	MCF7	HCT116
	Cell viability (% of control)		
2 10 μM	98 ± 2	97 ± 3	100 ± 2
100 μM	99 ± 3	98 ± 4	97 ± 5
4 10 μM	96 ± 3	97 ± 3	98 ± 4
100 μM	82 ± 4*	88 ± 4*	75 ± 5*

Values are the mean ± SD of two separate experiments carried out in triplicate.
* Significantly different from the relevant control with $P < 0.05$ (Student's *t*-test).

assessed compound was calculated by plotting the percentage viability versus concentration and reading off the concentration at which 50% of cells remained viable relative to the control. Each experiment was repeated at least three times in triplicate to obtain the mean values. In selected experiments, MTT test was carried out also on cells treated with the compounds for 48 or 72 h.

2.4.2. Measurement of phosphatidylserine exposure

The externalization of phosphatidylserine (PS) to the cell surface was detected by flow cytometry by double staining with Annexin V-FITC/PI. Phosphatidylserine, which is normally located on the cytoplasmic surface of cell membranes, is exposed on the cell surface upon induction of apoptosis. Annexin V binds to phosphatidylserine and is used to identify the earliest stage of apoptosis. PI, which does not enter cells with intact membranes, is used to distinguish between early apoptotic cells (Annexin V-FITC positive and PI negative) and late apoptotic cells (Annexin V-FITC/PI-double positive). Tumor cells (HepG2, MCF-7 and HCT116) were seeded in triplicate in 24-wells culture plates at a density of 5.0×10^4 cells/cm^2. After an overnight incubation, the cells were washed with fresh medium and incubated with the compounds in RPMI. After 24 h, cells were harvested by trypsinization and adjusted at 1.0×10^6 cells/ml with combining buffer according to the manufacturer's instructions (eBioscience, San Diego, CA). 100 μl of cell suspended solution was added to a new tube, and incubated with Annexin V-FITC and PI solution at room temperature in the dark for 15 min. Then samples of at least 1.0×10^4 cells were subjected to

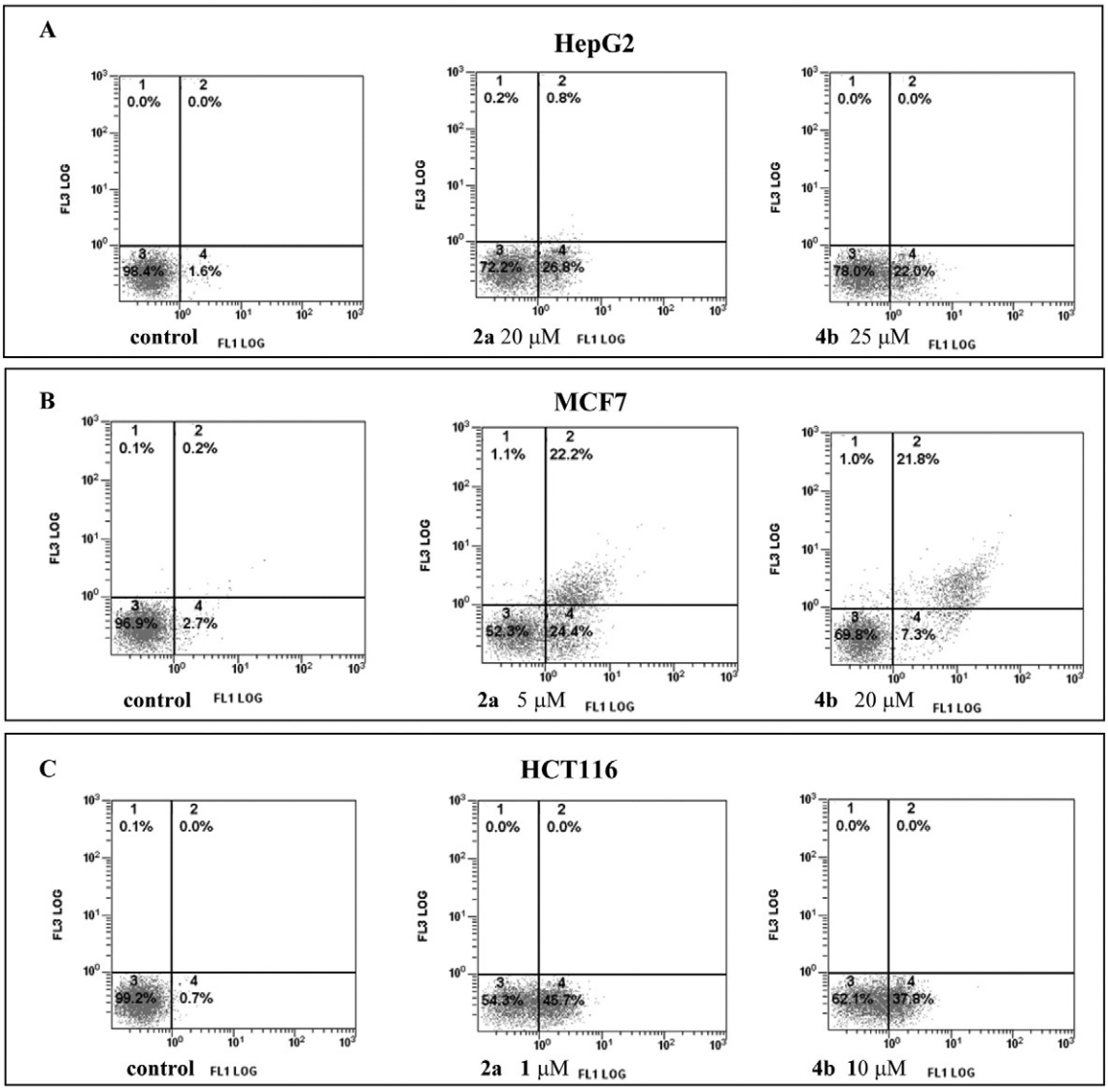

Fig. 4. Flow cytometric analysis for the quantification by AnnexinV/PI double staining of complexes **2a** or **4b** induced apoptosis in HepG2 (A), MCF-7 (B) and HCT116 (C). Cell monolayers were incubated for 24 h in the absence (control) or in the presence of individual complexes and submitted to double staining with Annexin V/PI as reported in *Experimental*. 3, viable cells (AnnexinV−/PI-); 4, cells in early apoptosis (AnnexinV+/PI-); 2, cells in tardive apoptosis (AnnexinV+/PI+); 1, necrotic cells (AnnexinV−/PI+). Representative images of three experiments with comparable results.

fluorescence-activated cell sorting (FACS) analysis by Epics XL™ flow cytometer using Expo32 software (Beckman Coulter, Fullerton, CA), using appropriate 2-bidimensional gating method.

2.4.3. Acridine orange and ethidium bromide morphological fluorescence dye staining

AO stains DNA bright green, allowing visualization of the nuclear chromatin pattern and stains both live and dead cells. EB stains DNA orange but is excluded by viable cells. Dual staining allows separate enumeration of populations of viable non apoptotic, viable (early) apoptotic, nonviable (late) apoptotic, and necrotic cells. Live cells appear uniformly green. Early apoptotic cells stain green and contain bright green dots in the nuclei as a consequence of chromatin condensation and nuclear fragmentation. Late apoptotic cells incorporate EB and therefore stain orange, but, in contrast to necrotic cells, the late apoptotic cells show condensed and often fragmented nuclei. Necrotic cells stain orange, but have a nuclear morphology resembling that of viable cells, with no condensed chromatin. Briefly, after tumor cells (HepG2, MCF-7 and HCT116) were treated with the compounds for 24 h, the medium was discarded. Cells were washed with saline 5 mM phosphate buffer (PBS) and then incubated with 100 μl PBS containing 100 μg/ml of EB plus 100 μg/ml of AO. After 20 s, EB/AO solution was discarded and cells immediately visualized by means of fluorescent microscope equipped with an automatic photomicrograph system (Leica, Wetzlar, Germany). Multiple photos were taken at randomly selected areas of the well to ensure that the data obtained are representative.

3. Results and discussion

3.1. IR spectra

The IR spectra of **2, 3, 4** and **5** free ligands show two characteristic bands due to ν(CH═N) of pyridine rings at ca. 1590 cm^{-1}, ν(C═N) at ca. 1630 of 1,2,4-oxadiazole [35,22], and at 1649–1665 of 1,2,4-triazole. The band of ν(C–F) vibration of perfluoroalkyl chains occurs at 1214–1150 cm^{-1} for the ligand **2**; and at 1223–1159 cm^{-1} for **3**. In 1,2,4-triazole ligands, the bands occur at 1240–1147 cm^{-1} for **4** and **5**. In the complexes, the bands are shifted at 1584 cm^{-1} ν(CH═N) and 1241–1144 cm^{-1} ν(C–F) for **2a** and at 1216–1157 cm^{-1} ν(C–F) for **3a** indicating that the ligands were present in the complexes; in fact the bands are shifted for complexation of the ligand to the platinum ion [35]. The presences of ν(Pt–Cl) at 342 and 326 cm^{-1} and at 333 e 320 cm^{-1} in the 2a and 3a complexes respectively, were due to Pt–Cl stretching vibrations. Moreover the observed bands at 279 and 256 cm^{-1} in **2a** and **3a** respectively, can be assigned to stretching vibrations of Pt–N bond [36–38]. The presence of non-coordinated molecules of solvate DMSO in both **2a** and **3a** is confirmed by a signal at 1023 cm^{-1} [38]. The vibration bands ν(CH═N) and ν(C–F) at ca 1590 cm^{-1} and at 1242–1147 cm^{-1} respectively confirmed the presence of the ligand in **4a**, **4b** and **5a** complexes. The spectra showed also symmetrical and asymmetrical stretching bands of Pt–Cl bond at 338, 312 cm^{-1} for **4a**, at 343, 320 cm^{-1} for **4b** and at 333, 322 cm^{-1} for **5a**, indicating a *cis*-square planar arrangement of the platinum(II) via chloride ions; ν(Pt-N) vibrations occur at 277, 272 and 271 cm^{-1} for **4a**, **4b** and **5a** respectively**.** In

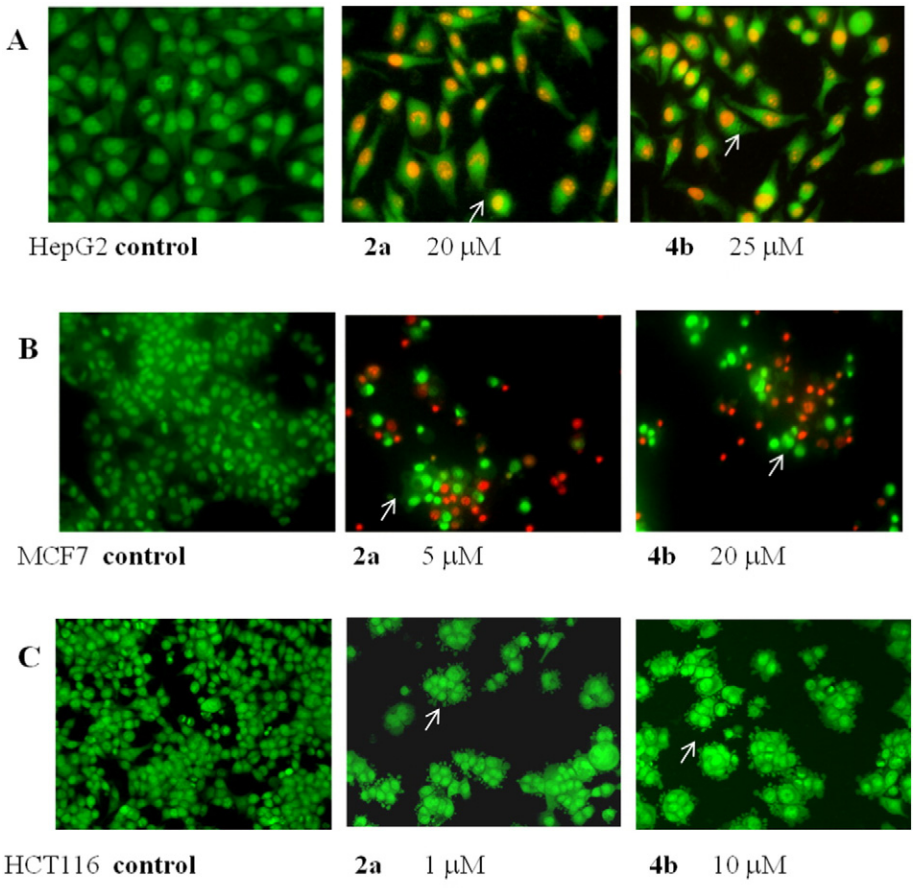

Fig. 5. Fluorescence micrographs of EB/AO double stained HepG2 (A), MCF-7 (B) and HCT116 (C) cells after treatment with complexes **2a** or **4b**. Cells were incubated for 24 h in the absence (control) or in the presence of individual complexes and submitted to double staining with EB/AO as reported in *Experimental*. Arrows indicate membrane blubbing. Representative images of three experiments with comparable results (200× magnification).

the complexes **4a** and **5a** the ν(S═O) vibrations were present for (solvate) DMSO in the range 1032–1037 cm^{-1} [39].

3.2. NMR spectra

The coordination mode of the complexes in solution was determined by using the ^1H NMR spectra and the assignments of resonances were based on literature data [40,9] and are in good agreement with proposed structure. The numbering of protons used for ^1H NMR is shown in Scheme 2. The four proton signals of pyridine coordinated to Pt(II) ion for **2a** and **3a** complexes are shifted downfield compared to the free ligands. In the ligands, signals are observed in the range 8.79–7.6 ppm for **2a** and at 8.85–7.72 ppm for **3a**; in the first and second complex doublets are assigned to $C_{6'}H$ and $C_{3'}H$ and double of triplet and multiplet to $C_{5'}H$ and $C_{4'}H$ respectively. Therefore the coordination of the ligand can be ascribed to the N1 atom of pyridine acting as monodentate, being the proton $C_{6'}H$ the most shifted, as reported for similar complexes with Mn(II) and Co(II) ions [41]. The presence of a singlet for **2a** at 2.65 ppm and for **3a** at 2.53 ppm close to the solvent DMSO-d_5 multiplet is attributed to the non-coordinated (solvate) DMSO [39]. The ^1H NMR resonances of **4a**, **4b** and **5a** complexes show a slight shift to down field of pyridine protons as compared to the uncoordinated ligands **4** and **5**. The doublet at 8.85 ppm can be attributed to the proton $C_{6'}H$ for **4a** and **4b** complexes and it is slightly shifted as compared with the proton $C_{6'}H$ (8.80 ppm) of the free ligand. Another doublet at 8.22 ppm can be assigned to proton $C_{5'}H$, while two triplets for **4a** and two doublet of triplets for **4b** at 8.11 and 7.68 ppm, can be assigned to $C_{3'}H$ and $C_{4'}H$ respectively. The singlet at 4.44 ppm of the methyl group of 1,2,4-triazole is also slightly shifted compared to uncoordinated ligand (4.39 ppm). The presence in **4a** of a singlet signal in the range 2.61–2.57 is due to non-coordinated DMSO. Coordination of Pt(II) ion to the ligand for **4a**, occurs via N2 atoms of two 1,2,4-triazole moieties and its coordination is completed by $PtCl_2$ moiety. On the contrary for **4b** only one molecule of 1,2,4-triazole is coordinated to Pt(II) ion via N4 atom of triazole and N1 atom of pyridine, where the remaining two coordination sites of the platinum are engaged with two chlorine atoms. Similar complexes with 6-(5-trifluoromethyl-1,2,4-triazol-3yl)-4,4′-dimethyl-2,2′-bipyridine ligand have been reported [42]. In the complex **4a** and **5a** the coordination environment of Pt(II) ion is equal and the resonance signals of the pyridine protons are not shifted with respect to the ligand and they occur in the range 8.80–7.62 ppm.

3.3. Biology

Cytotoxicity in vitro of the synthesized platinum(II) complexes was evaluated by MTT on three tumor human cell lines: HepG2, HTC116 and MCF-7. After 24 h of incubation, a clear dose dependent inhibitory effect of **2a** and **4b** on the viability of all the studied cancer cell lines was measured, whereas far less cytotoxicity of **3a**, **4a** and **5a** was noticeable (Fig. 1). Prolonged incubation times (48–72 h) with **2a** and **4b** resulted in a progressive cell growth inhibition, indicating antiproliferative activity of the compounds (Fig. 2). Table 1 reports the concentration of **2a** and **4b** required to inhibit 50% of cell proliferation after 24 h of treatment, when compared to untreated cells (IC_{50}), in comparison with cisplatin assayed in the same experimental conditions. The calculated IC_{50} values show that anti-proliferative activity of both the cisplatin analogs was comparable to that observed with cisplatin, being **2a** significantly more efficacy than **4b** against all the selected cancer cells. Under identical conditions, both the platinum(II) complexes did not substantially impaired viability of intestinal normal-like differentiated Caco-2 cells, suggesting high selectivity towards tumor cells (Fig. 3). Eventual contribution of the ligand to the cytotoxic activity of **2a** and **4b** was assessed by MTT after treatment for 24 h of the tumor cell lines with **2** or **4**, respectively, at 10 and 100 μM. While **2** did not affect cell viability at any assayed concentration, a slight but significant decrement ($P < 0.05$) of the cell proliferation of all selected tumor lines was measured with compound **4** at 100 μM (Table 2). Mechanism of the anti-proliferative effect (necrosis or apoptosis) of **2a** and **4b** was investigated by double staining with PI and Annexin V-FITC followed by cytofluorimetric analysis. The chosen concentrations were selected on the basis that they represented the IC_{50} values measured at 24 h for each cell line, as reported in Table 1. Fig. 4 shows that both the compounds did not exert necrotic effects in any cancer cell line, while induced a clear shift of viable cells towards early apoptosis in HepG2 and HCT116 or towards late apoptosis in MCF-7 cells. To confirm apoptotic mechanism of cytotoxicity of the studied platinum(II) complexes, we carried out morphological evaluation of the HepG2, HCT116 and MCF-7 tumor cells using AO and EB double staining. After 24 h of treatment with **2a** or **4b** at IC_{50} concentration, fluorescent microscopy revealed the appearance of cells containing bright green patches in the nuclei as a consequence of chromatin condensation and nuclear fragmentation, which are typical features of apoptosis. Moreover, fluorescing orange cells owing to increase of cell permeability to ethidium bromide, cell shrinkage and nuclear fragmentation were also evident as cells in late apoptosis, chiefly in MCF-7 cell line (Fig. 5). Taken together, these findings provided strong evidence that both the cisplatin analogs induced apoptosis in the studied tumor cell lines.

4. Conclusions

The ligands 5-perfluoroalkyl-1,2,4-oxadiazole and 3-perfluoroalkyl-1,2,4-triazole and their metal complexes **2a**, **3a**, **4a**, **4b**, **5a** with Pt(II) ion have been synthesized and characterized by the combination of elemental analysis, atomic absorption spectrometer, ^1H NMR, IR, and molar conductivities. In the complexes **2a** and **3a**, the ligands 5-perfluoroalkyl-1,2,4-oxadiazole bind to Pt(II) ion in a monodentate way through the pyridine ring where the geometry of metal is square planar. In **4a** and **5a** the 3-perfluoroalkyl-1,2,4-triazole ligands also act as monodentate to Pt(II) ion through N2 atom of the 1,2,4-triazole ring. Instead, in **4b** the coordination of the ligand to the metal ion occurs in a bidentate mode. The five new complexes and their new ligands synthesized have been tested in vitro. The complexes **2a** and **4b** and only one ligand **2** were found to be active towards the engaged three tumor cell lines, but **2a** was found to be much more active than its ligand **2**. A tentative examination of a qualitative structure–activity relationship indicates that the biological activity of the new family of Pt(II) complexes depends on the length of the perfluoroalkyl chain; in fact, the most active complexes are those with **pfhop** and **pfhtp** ligands; this fact could be ascribed to an enhanced lipophilicity of the longest perfluoroalkyl chain that could affect the cell membrane permeation. The geometry of Pt(II) is square-planar and the planarity of the complexes was suggested to be essential for antitumor activity, and probable intercalation with DNA [43]; this fact could suggest an explanation for the lack of bioactivity of complexes **4a** and **5a**, that being more hindered, twist the planarity of the complex.

Furthermore, the complex **4b** with respect to **4a** has only one ligand moiety, so that around Pt(II) ion there is less steric hindrance, therefore **4b** is more available to the formation of DNA binding.

Acknowledgments

Financial support by the Università di Palermo (FFR 2012-2013-ATE 0291) is gratefully acknowledged.

Appendix A. Supplementary data

Supporting Information: ^1H NMR spectra for compounds 2–5 are reported in Figs. S1–S4, GC–MS chromatogram and MS spectra associated for compounds 2–5 are reported in Figs. S5–S8 respectively. Supplementary data associated with this article can be found in the online version, at doi: http://dx.doi.org/10.1016/j.jinorgbio.2015.11.020.

References

[1] J. Zhao, S. Gou, Y. Sun, L. Fang, Z. Wang, Inorg. Chem. 51 (2012) 10317–10324.
[2] P. Marqués-Gallego, H. den Dulk, J. Brouwer, S. Tanase, I. Mutikainen, U. Turpeinen, J. Reedijk, Biochem. Pharmacol. 78 (2009) 365–373.
[3] J. Reedijk, Platin. Met. Rev. 52 (2008) 2–11.
[4] C. Molenar, J.M. Teuben, R.J. Heetebrij, H.J. Tanke, J. Reedijk, J. Biol. Inorg. Chem. 5 (2000) 655–665.
[5] P. Marqués-Gallego, G.V. Kalayda, U. Jaehde, H. den Dulk, J. Brouwer, J. Reedijk, J. Inorg. Biochem. 103 (2009) 791–796.
[6] L. Arzuman, P. Beale, J.Q. Yu, F. Huq, Anticancer Res. 35 (2015) 2783–2794.
[7] J.H. Guo, J. Chen, C.P. Li, M. Du, J. Mol. Struct. 975 (2010) 147–153.
[8] D. Schweinfurth, S. Strobel, B. Sarkar, Inorg. Chim. Acta 374 (2011) 253–260.
[9] S. Rubino, P. Portanova, A. Albanese, G. Calvaruso, S. Orecchio, G. Fontana, G.C. Stocco, J. Inorg. Biochem. 101 (2007) 1473–1482.
[10] S. Buscemi, A. Pace, A. Palumbo Piccionello, I. Pibiri, N. Vivona, Heterocycles 63 (2004) 1619–1628.
[11] A. Palumbo Piccionello, A. Pace, I. Pibiri, S. Buscemi, N. Vivona, Tetrahedron 62 (2006) 8792–8797.
[12] A. Pace, P. Pierro, Org. Biomol. Chem. 7 (2009) 4337–4348.
[13] J. Bostrom, A. Hogner, A. Llinas, E. Wellner, A.T. Plowright, J. Med. Chem. 55 (2012) 1817–1830.
[14] A. Palumbo Piccionello, R. Musumeci, C. Cocuzza, C.G. Fortuna, A. Guarcello, P. Pierro, A. Pace, Eur. J. Med. Chem. 50 (2012) 441–448.
[15] L. Lentini, R. Melfi, A. Di Leonardo, A. Spinello, G. Barone, A. Pace, A. Palumbo Piccionello, I. Pibiri, Mol. Pharm. 11 (2014) 653–664.
[16] I. Pibiri, L. Lentini, R. Melfi, G. Gallucci, A. Pace, A. Spinello, G. Barone, A. Di Leonardo, Eur. J. Med. Chem. 101 (2015) 236–244.
[17] I. Pibiri, A. Pace, S. Buscemi, V. Causin, F. Rastrelli, G. Saielli, Phys. Chem. 14 (2012) 14306–14314.
[18] F. Lo Celso, I. Pibiri, A. Triolo, R. Triolo, A. Pace, S. Buscemi, N. Vivona, J. Mater. Chem. 17 (2007) 1201–1208.
[19] A. Palumbo Piccionello, A. Guarcello, A. Calabrese, I. Pibiri, A. Pace, S. Buscemi, Org. Biomol. Chem. 10 (2012) 3044–3052.
[20] I. Pibiri, A. Palumbo Piccionello, A. Calabrese, S. Buscemi, N. Vivona, A. Pace, Eur. J. Org. Chem. (2010) 4549–4553.
[21] F.S. Palumbo, M. Di Stefano, A. Palumbo Piccionello, C. Fiorica, G. Pitarresi, I. Pibiri, S. Buscemi, G. Giammona, RSC Adv. 4 (2014) 22894–22901.
[22] H.M. Coley, J. Sarju, G. Wagner, J. Med. Chem. 51 (2008) 135–141.
[23] I. Pibiri, S. Buscemi, Curr. Bioact. Compd. 6 (2010) 208–242.
[24] S. Komeda, M. Lutz, A.L. Spek, Y. Yamanaka, T. Sato, M. Chikuma, J. Reedjik, J. Am. Chem. Soc. 124 (2002) 4738–4746.
[25] M.A. Girasolo, L. Canfora, P. Sabatino, D. Schillaci, E. Foresti, S. Rubino, G. Ruisi, G. Stocco, J. Inorg. Biochem. 106 (2012) 156–163.
[26] S. Rubino, V. Di Stefano, A. Attanzio, L. Tesoriere, M.A. Girasolo, F. Nicolò, G. Bruno, S. Orecchio, G.C. Stocco, Inorg. Chim. Acta 418 (2014) 112–118.
[27] M.A. Girasolo, A. Attanzio, P. Sabatino, L. Tesoriere, S. Rubino, G. Stocco, Inorg. Chim. Acta 423 (2014) 168–176.
[28] J.H. Price, A.N. Williamson, R.S. Schramm, B.B. Wayland, Inorg. Chem. 11 (1972) 1280–1284.
[29] K. Gobis, H. Foks, A. Kedzia, M. Wierzbowska, Z. Zwolska, J. Heterocycl. Chem. 46 (2009) 1271–1279.
[30] W. Schöniger, Mikrochim. Acta 43 (1955) 123–129.
[31] I. Pibiri, A. Pace, A. Palumbo Piccionello, P. Pierro, S. Buscemi, Heterocycles 68 (2006) 2653–2661.
[32] I. Pibiri, A. Pace, S. Buscemi, N. Vivona, L. Malpezzi, Heterocycles 68 (2006) 307–321.
[33] W.J. Geary, Coord. Chem. Rev. 7 (1971) 81–122.
[34] D. Sun, H. Lennernas, L.S. Welage, J.L. Barnett, C.P. Landowski, D. Foster, D. Fleischer, K.D. Lee, J.L. Amidon, Pharm. Res. 19 (2002) 1400–1416.
[35] A. Nadezhda, A. Bokach, M.L. Kuznetsov, M. Haukka, V.I. Ovcharenko, E.V. Tretyakov, V.Y. Kukushkin, Organomet 28 (2009) 1406–1413.
[36] I. Łakomska, B. Golankiewicz, J. Wietrzyk, M. Pełczyńska, A. Nasulewicz, A. Opolski, J. Sitkowski, L. Kozerski, E. Szłyk, Inorg. Chim. Acta 358 (2005) 1911–1917.
[37] S.G. de Almeida, J.L. Hubbard, N. Farrell, Inorg. Chim. Acta **1**93 (1992) 149–157.
[38] K. Nakamoto, Infrared and Raman Spectra of Inorganic and Coordination Compounds, Part B: Applications in Coordination, Organometallic and Bioinorganic Chemistry, 5th Ed. A Wiley-Interscience Publ., U.S.A., 1997
[39] J. Jolley, W.I. Cross, R.G. Pritchard, C.A. McAuliffe, K.B. Nolan, Inorg. Chim. Acta 315 (2001) 36–43.
[40] N.I. Dodoff, D. Kovala-Demertzi, M. Kubiak, J. Kuduk-Jaworska, A. Kochel, G.A. Gorneva, Z. Naturforsch. 61b (2006) 1110–1122 (and reference therein).
[41] A. Terenzi, G. Barone, A. Palumbo Piccionello, G. Giorgi, A. Guarcello, A. Pace, Inorg. Chim. Acta 373 (2011) 62–67.
[42] J.L. Chen, X.X. Chen, X.Z. Tan, J.Y. Wang, X.F. Fu, L.H. He, Y. Li, G.Q. Zhong, H.R. Wen, Inorg. Chem. Commun. 35 (2013) 96–99.
[43] S. Rubino, S. Petruso, R. Pierattelli, G. Bruno, G.C. Stocco, L. Steardo, M. Motta, M. Passerotto, E. Del Giudice, G. Gulì, J. Inorg. Biochem. 98 (2004) 2071–2079.